

Structure-properties relationship in polymer nanocomposites based on polylactic acid and carbon nanotubes

E.A. Lysenkov¹, V.L. Demchenko², M.M. Lazarenko³

¹Petro Mohyla Black Sea National University, 54003, 68 Desantnykyv St., 10, Mykolaiv, Ukraine

²E.O. Paton Electric Welding Institute of the National Academy of Sciences of Ukraine 03150, 11 Kazymyr Malevich St., Kyiv, Ukraine

³Taras Shevchenko National University of Kyiv, Faculty of Physics, 03022, 2 Academician Glushkov Ave., Kyiv, Ukraine

Received April 24, 2025

The work investigated the effect of carbon nanotubes (CNTs) on the properties of polylactic acid. It was found that the addition of CNTs does not alter the chemical structure of the polymer, but substantially influences its crystallinity, thermophysical, conductive and mechanical characteristics. Analysis of structural features showed the absence of new chemical bonds, but structural ordering of the matrix and changes in morphology were recorded. It is shown that the degree of crystallinity and melting temperature increase with a CNT content of up to 0.6%, and decrease when this value is exceeded. The electrical conductivity increases significantly after reaching the percolation threshold (0.5%), which indicates the formation of a conductive network. The mechanical properties show a nonlinear dependence with a minimum at a content of 0.5% CNT due to the agglomeration of nanotubes. The results obtained indicate the need to optimize the composition of the composite to achieve the desired characteristics.

Keywords: Polymer nanocomposites; Polylactic acid; Carbon nanotubes; Degree of crystallinity; Percolation.

Зв’язок між структурою та властивостями в полімерних нанокомпозитах на основі полімолочної кислоти та вуглецевих нанотрубок.
С.А. Лисенков, В.Л. Демченко, М.М. Лазаренко

У роботі досліджено вплив вуглецевих нанотрубок (ВНТ) на властивості полілактиду (ПЛА). Встановлено, що додавання ВНТ не змінює хімічну структуру полімеру, але суттєво впливає на його кристалічність, теплофізичні, електропровідні та механічні характеристики. Аналіз структурних особливостей засвідчив відсутність нових хімічних зв’язків, однак зафіксовано впорядкування матриці та зміну морфології. Показано, що за вмісту ВНТ до 0,6 % зростає ступінь кристалічності та температура плавлення, а при перевищенні цього значення відбувається їх зниження. Електропровідність різко зростає після досягнення порогу перколяції (0,5 %), що свідчить про формування провідної сітки. Механічні властивості демонструють нелінійну залежність з мінімумом при 0,5 % ВНТ, обумовленим агломерацією нанотрубок. Отримані результати вказують на необхідність оптимізації складу композиту для досягнення бажаних характеристик.

1. Introduction

Polymer nanocomposites have attracted considerable attention due to their potential use as

materials with improved properties. Polylactic acid (PLA) nanocomposite filled with carbon nanotubes (CNT) is one of the promising materials due to its lightness, biodegradability and

excellent electrical properties [1]. The introduction of CNTs into the matrix of the PLA leads to percolation phenomena, which significantly affect the functional properties of the nanocomposite [2].

With increasing concentration of CNTs, a critical threshold is reached, known as the percolation threshold, after which the material changes from a non-conducting to a conducting state [3, 4]. Most polymer-CNT systems have a low percolation threshold value [5, 6]. For example, a number of studies have shown that the introduction of CNTs into PLA leads to a significant improvement in electrical conductivity, and the percolation threshold depends on factors such as the aspect ratio and dispersion of the CNTs [7-9].

The structure of PLA-CNT nanocomposites plays a decisive role in their functional properties. The directional or random distribution of CNTs in the PLA matrix can significantly affect the formation of a percolation network within the polymer matrix [10, 11]. In addition, CNT parameters, such as aspect ratio, play a key role; higher aspect ratios usually lead to lower percolation thresholds and improved dielectric properties [12, 13].

The enhancement of electrical properties in PLA-CNT nanocomposites is primarily attributed to the conductive nature of carbon nanotubes. When CNTs are added to PLA, their high aspect ratio facilitates the formation of conductive pathways within the polymer matrix, leading to a significant increase in electrical conductivity. For instance, Zhang et al. reported that the introduction of CNTs leads to a step-like change in the electrical conductivity of PLA-based nanocomposites [14]. In this case, percolation behavior is observed, and the percolation threshold value for such systems was 1.45%. It is also reported in this work that MWCNTs, acted as nucleating agent and accelerated the crystallization process of composites. Beltrán et al. explained that electrical conductivity in these composites can reach substantial levels depending on the volume fraction of CNTs used, highlighting the potential of the material for electronic applications [15]. Additionally, it has been shown that CNTs can induce a percolation threshold, affecting the thermal properties of composites by altering their crystallinity [16].

The mechanical performance of PLA-CNT nanocomposites typically reflects considerable enhancements over pure PLA due to the effec-

tive stress transfer between the CNTs and the polymer matrix. Several studies, including that of Mohan et al., have shown that the addition of CNTs can lead to increased tensile strength and elastic modulus, which is critical for structural applications [17].

Therefore, establishing the percolation threshold and studying the system properties near the percolation threshold is a key issue in the development of CNT-based nanocomposites. The behavior of properties near the percolation threshold and its correlation with the structural features is crucial for optimizing the functional characteristics of PLA-CNT nanocomposites for their further practical application. In this work, the correlation between structure and properties of PLA-CNT nanocomposites is investigated.

2. Experimental

2.1. Materials

Polylactic acid (PLA), manufactured by Devil Design (Poland), was selected as the polymer matrix. At $T = 20$ °C, PLA is a solid with a density of $\rho = 1250$ kg/m³. Before use, the polymer was dehydrated by heating for four hours at 80 °C.

Multi-walled CNTs manufactured by "Spetsmash", LTD (Ukraine) were made of ethylene by chemical vapor deposition. The content of mineral impurities was no more than 0.1%. Fig. 1 shows transmission electron microscope micrographs of carbon nanotubes used in this study. According to the manufacturer, the specific surface area is 190 m²/g, the outer diameter is 15 nm, the length is (5÷10) μm, the aspect ratio $L/d \approx 250 \pm 170$, and the density of CNTs is $\rho = 2045$ kg/m³.

2.2. Preparation of nanocomposites

To prepare the materials for the study, the polymer was dissolved in a mixture of solvents of dimethyl sulfoxide and dimethylacetamide (1:1). In this case, a 10% solution of the polymer was prepared. Nanocomposites were prepared by ultrasonic mixing in the polymer solution using an ultrasonic disperser UZD A-650 (Ukraine). Dispersion continued for 5 min at a frequency of 22 kHz, the ultrasound power was 300 W. The CNT content was varied within (0.1 ÷ 1.5) wt. %. (hereinafter %). After ultrasonic treatment, the resulting mixture was poured onto a glass surface and dried until the solvents were completely removed at a temperature of 80-100 °C.

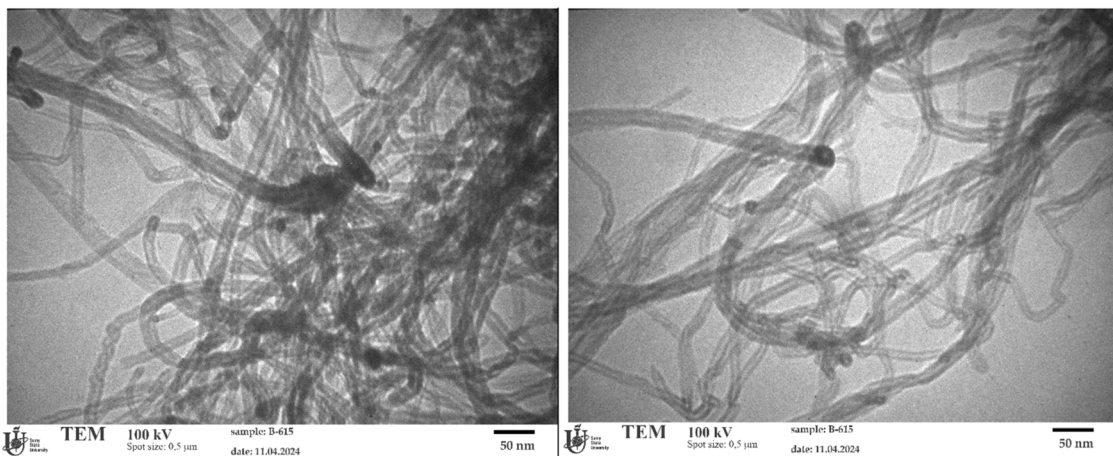


Fig. 1. Photographs of carbon nanotubes

2.3. Experimental

Microphotographs of polymer-CNT systems were obtained using a Sigeta optical microscope equipped with a digital video eyepiece DMC-800 and an image processing system. The samples were placed in a glass cell with a thickness of 80 μm .

FTIR spectra of the samples were obtained using a Shimadzu IR Tracer-100 spectrometer, equipped with a QATR 10 Single-Reflection ATR with a Diamond Crystal, operating with a resolution of 0.5 cm^{-1} in the mid-IR spectral range (4000–400 cm^{-1}). The spectra were acquired in adsorption mode using 28 scans for each sample.

The structure of the obtained samples was investigated by the method of wide-angle X-ray diffraction on an XRD-7000 diffractometer (Shimadzu, Japan), using CuK_α radiation ($\lambda = 1.54 \text{ \AA}$) and a graphite monochromator. The measurements were carried out in automatic step-scanning mode at $U = 30 \text{ kV}$, $I = 30 \text{ mA}$ in the scattering angle range from 3.0 to 80 degrees, the exposure time was 5 s.

The temperature dependence of the heat flow was studied in a dry nitrogen atmosphere in the temperature range from 20 $^\circ\text{C}$ to 200 $^\circ\text{C}$ at a heating rate of 5 $^\circ\text{C}/\text{min}$ using differential scanning calorimetry (DSC) on a DSC-60 Plus device (Shimadzu, Japan). The thermophysical characteristics of DSC curves were analyzed using LabSolutions TA Software. It allows localization of the endothermic peak indicating the melting process. The melting point (T_m) is then defined as the peak maximum temperature. The absolute error in determining the melting temperature is 0.1 $^\circ\text{C}$.

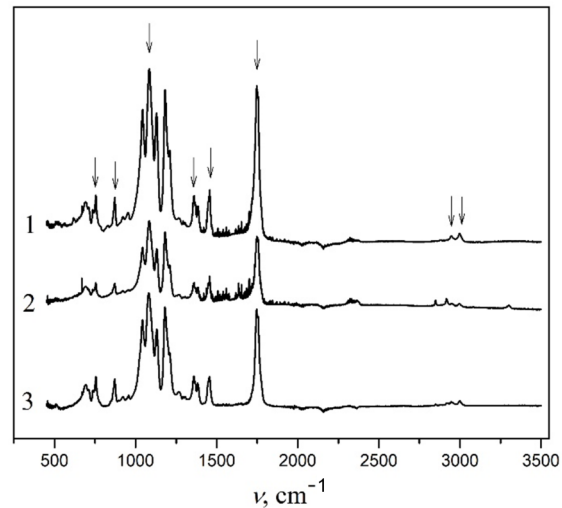


Fig. 2. FTIR spectra for unfilled polyactic acid (1) and nanocomposites containing 0.5% (2) and 1.5% (3) CNTs

The electrical conductivity was studied by impedance spectroscopy using an E7-20 impedance meter. The sample was placed between the electrodes of the cell, after which its real (Z) and imaginary (Z'') parts of the impedance were subsequently measured. Based on the obtained dependencies of the complex impedance, the electrical conductivity at direct current was determined as $\sigma_{DC} = d/SR_{DC}$, where: S is the sample area; d is the sample thickness. Measurements were carried out at room temperature in the frequency range of 25 Hz – 2 MHz. R_{DC} was determined from Nyquist diagrams ($Z''(Z)$).

Mechanical tests of the obtained systems were carried out under uniaxial tension on an AGS-10kNX testing machine (Shimadzu, Japan) at a linear speed of 50 mm/min. To increase the accuracy of the measurements, they

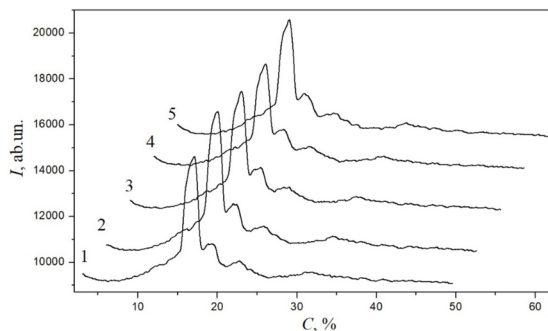


Fig. 3. Wide-angle X-ray scattering curves for unfilled PLA (1) and nanocomposites containing 0.25% (2), 0.5% (3), 1% (4) and 1.5% (5) CNTs.

were carried out three times with subsequent averaging of the results.

3. Results and discussion

3.1. Structural features of PLA-CNT-based materials

Fig. 2 shows the FTIR spectra of unfilled polylactic acid (PLA) and nanocomposites containing CNTs. The following characteristic peaks are observed in the IR spectrum of PLA: one of the strongest and most pronounced peaks is at 1746 cm^{-1} , corresponding to the stretching vibrations of the carbonyl group ($\text{C}=\text{O}$) in the ester bonds that comprise it; a group of peaks at $1180\text{--}1260\text{ cm}^{-1}$, corresponding to the asymmetric and symmetric vibrations of the $\text{C}-\text{O}-\text{C}$ bonds in the fragments of the polyether chain; peaks of deformation vibrations of the CH_3 groups (methyl groups) at 1452 and 1351 cm^{-1} , which are part of the side radicals of polylactic acid; weaker maxima at 2995 and 2946 cm^{-1} , corresponding to C-H stretching vibrations in CH and CH_3 groups; weak peaks at 868 and 754 cm^{-1} , attributed to vibrations of different types of C-C bonds and, possibly, vibrations associated with the structural features of the amorphous and crystalline phases of polylactic acid [18]. These absorption bands are typical for most polylactic acid-based systems [19].

Analyzing the curves for PLA-CNT nanocomposites, we can see that they have the same absorption peaks as the curve for unfilled polylactic acid. This suggests that no new bonds or strong chemical interactions are formed in the nanocomposites.

The diffraction patterns (Fig. 3) for systems based on PLA and CNT show that all the studied systems are partially crystalline, as evidenced by the presence of intense peaks. The proportion of the crystalline phase can be estimated by calculating the relative degree of crystallinity using equation (1) [20]:

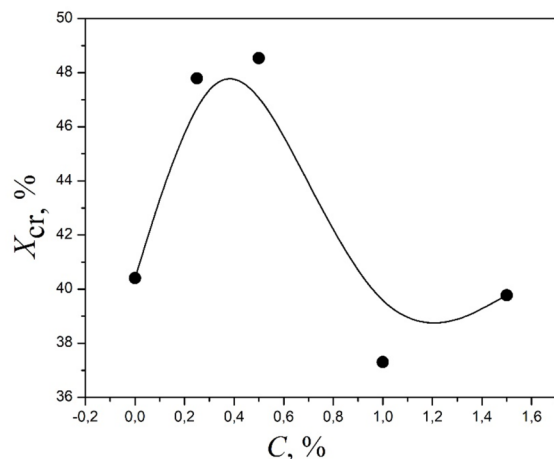


Fig. 4. Dependence of the relative degree of crystallinity on the content of carbon nanotubes for polylactic acid-based nanocomposites.

$$\chi_{cr} = \frac{Q_{cr}}{Q_{cr} + Q_{am}} \cdot 100\% , \quad (1)$$

where Q_{cr} is the area of the diffraction peak, which characterizes the crystal structure of the amorphous-crystalline polymer, $(Q_{cr} + Q_{am})$ is the total area of the diffraction peak.

The values of the relative degree of crystallinity depending on the content of carbon nanotubes for polylactic acid-based nanocomposites are shown in Fig. 4. It is seen that carbon nanotubes significantly affect the structure of the polymer matrix. When introducing CNTs into PLA, the degree of crystallinity changes unevenly: it increases in the concentration range from 0 to 0.6%, reaching a maximum at 0.6% CNTs; then, in the concentration range (0.6%–1%) a decrease in the degree of crystallinity to the level of unfilled PLA is observed. This behavior can be explained as follows. CNTs can act as nucleating agents, contributing to the nucleation of crystalline regions of the polymer matrix. This leads to an increase in the degree of crystallinity of PLA at low concentrations of nanotubes (concentration range up to 0.6%). However, with an increase in the CNT content, a decrease in crystallinity is possible due to agglomeration of nanotubes and limitation of the mobility of polymer chains.

3.2. The influence of CNT content on the thermophysical characteristics of PLA-based materials

Fig. 5 shows the DSC curves obtained as a result of the first heating for PLA-CNT systems. The first heating graphs record temperature transitions reflecting the structure of the material formed during the manufacturing and stor-

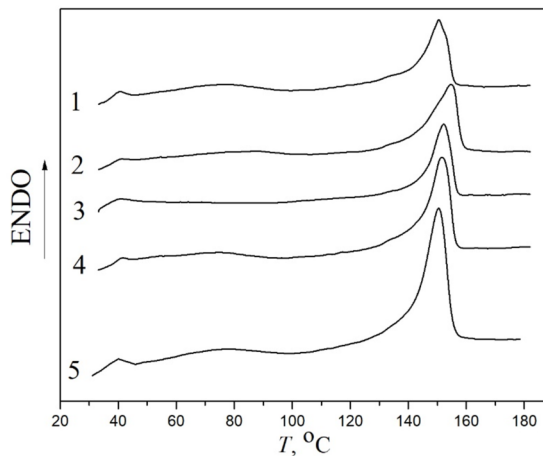


Fig. 5. DSC curves for systems based on PLA (1) filled with 0.25% (2), 0.5% (3), 1% (4) and 1.5% (5) CNTs.

age of the samples. PLA and its nanocomposites are characterized by a melting transition temperature T_m , associated with the destruction of crystalline regions formed during the manufacturing of materials. In this state, the material retains residual crystallinity, which is determined by the cooling conditions after processing. Figure 6 shows the dependences of melting temperatures and the degree of crystallinity on the content of nanotubes.

The melting temperature and degree of crystallinity of polylactic acid exhibit a characteristic nonlinear dependence with increasing carbon nanotube content. In the CNT concentration range from 0% to 0.5%, an increase in these parameters is observed, whereas with a further increase in the nanofiller content, they decrease to values close to the initial ones.

The increase in the melting temperature and degree of crystallinity at low CNT concentrations may be due to the action of nanotubes as nucleation centers [21]. CNTs contribute to the ordering of PLA macromolecular chains, which facilitates their packing into crystalline domains and increases the energy barrier for melting. However, with a CNT content exceeding 0.5%, agglomeration of nanotubes occurs, which reduces their effective interaction with the polymer matrix. This leads to the formation of defects in the crystal structure, a decrease in the degree of crystallinity and a corresponding decrease in the melting temperature.

The obtained results are consistent with the known phenomena characteristic of polymer nanocomposites containing CNTs [22] and confirm the importance of optimal selection of the nanofiller concentration to achieve improved physical and mechanical characteristics of the polymer material.

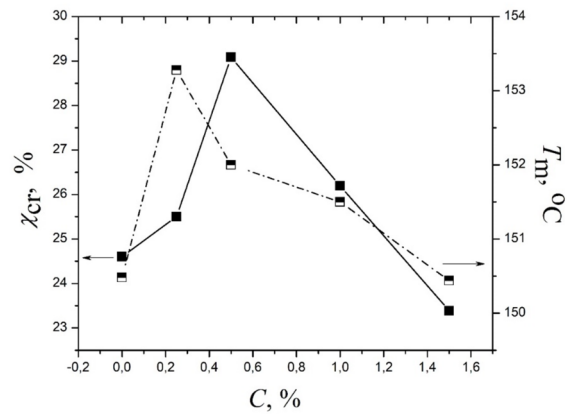


Fig. 6. Dependences of the degree of crystallinity and melting temperature on the content of carbon nanotubes for polylactic acid-based nanocomposites.

3.3. Effect of CNT content on electrical conductivity of PLA-based materials

Fig. 7 shows the dependence of electrical conductivity at constant current σ_{DC} on CNT concentration for the studied polylactic acid-CNT systems. The graph exhibits the percolation behavior typical of nanocomposite systems containing conductive fillers. It is seen that at a low CNT content ($\sim 0.4\%$) the value of σ_{DC} remains extremely low ($\leq 10^{-11} \text{ S/cm}$) corresponding to the dielectric nature of the polymer matrix. However, with an increase in the CNT content, starting from $\sim 0.5\%$, a sharp increase in electrical conductivity by several orders of magnitude is observed, which indicates the formation of a percolation network of conductive particles in the PLA matrix. This dependence is well described by the classical percolation model, where the electrical conductivity changes according to a power law [23]:

$$\sigma_{DC} = \sigma_m (C - C_c)^t \quad \text{for } C > C_c, \quad (2)$$

where σ_{DC} , σ_m are electrical conductivities of the composite and matrix, respectively; C_c is the percolation threshold, i.e. the lowest filler content at which a continuous cluster of particles is formed; t is the critical conductivity exponent.

The percolation behavior of PLA-CNT nanocomposites was analyzed using equation (2). The percolation threshold (C_c) is defined as 0.5%, and the critical conductivity exponent above this threshold is $t = 3.3$.

The percolation threshold of 0.5% observed in PLA-CNT nanocomposites is relatively low, indicating the effective formation of an electrically conductive network with minimal CNT filling. This value is close to or even lower than

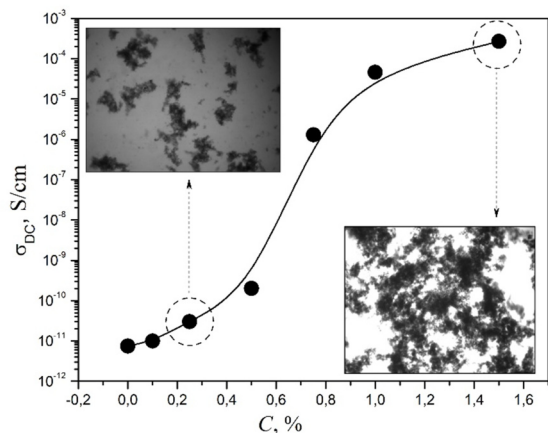


Fig. 7. Concentration dependence of electrical conductivity at direct current for systems based on polylactic acid and CNTs. The insets show micrographs of the systems obtained at a magnification $\times 100$.

the threshold values obtained for other polymer-carbon nanotube composites. For similar systems, C_c value typically ranges from 0.1 to 1% and depends on factors such as CNT dispersion, aspect ratio, and polymer-CNT interaction. For example, polyethyleneglycol-CNT and polypropyleneglycol-CNT systems are often characterized by percolation threshold values in the range of 0.4–0.6% [24].

3.4. Effect of CNT content on mechanical properties of PLA-based materials

Fig. 8 shows the concentration dependences of tensile strength and elongation at break for PLA-CNT systems. It can be seen that these parameters exhibit extreme behavior: they decrease, reach a minimum, and then increase with increasing CNT content in the system. This behavior of mechanical parameters is often observed in polymer-filler systems and can be explained by several factors, namely dispersion, interfacial interaction and stress transfer mechanisms. At very low CNT content, up to 0.5–1%, nanotubes tend to agglomerate due to strong Van der Waals forces between filler particles. Instead of improving mechanical properties, agglomerates create weak points in the matrix, causing microcracks under load [25]. That is, in the concentration range from 0 to ~1% CNT, the negative effect of agglomeration and poor dispersion dominates, which causes a drop in tensile strength. The minimum at 1% CNT is the result of these competing effects, when the system has not yet transitioned to effective strengthening [26].

When the CNT content is above 1%, the system forms a percolation network of filler par-

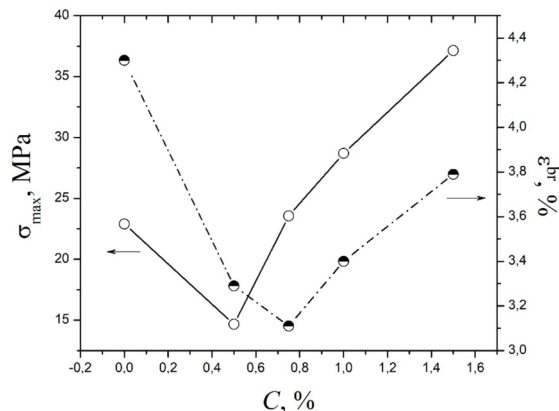


Fig. 8. Dependence of tensile strength and elongation at break on the nanotube content for polylactic acid-based systems

ticles and their aggregates, which improves load transfer and strengthens the composite [27]. The interconnected network of CNTs can bridge cracks and prevent their propagation, leading to increased tensile strength.

The differences in the concentration dependences of various characteristics for the polylactic acid-nanotube system, shown in Figs. 4, 6, 7 and 8, are associated with different mechanisms of the influence of nanotubes on these characteristics. For systems containing carbon nanotubes, percolation processes (formation of a non-permeable cluster of CNTs, which permeates the entire volume of the material) are observed. In this case, a sharp change in properties, for example, electrical conductivity, is observed (Fig. 7). A sharp increase in electrical conductivity does not always require the formation of direct contacts between CNTs; it is sufficient to bring them closer to a “tunnel” distance. For the beginning of a change in structural characteristics, for example, the degree of crystallinity, the formation of direct contacts between CNTs is also not necessarily required. The degree of crystallinity increases when individual CNTs and their small clusters act as nucleating agents and accelerate crystallization (Fig. 4 and 6). However, for the mechanical characteristics of systems based on polylactic acid, the formation of direct contacts between CNTs plays a decisive role, when they form a strong network with a reinforcing effect (Fig. 8). That is why an increase in some characteristics is observed at lower CNT concentrations, and an increase in mechanical characteristics at higher concentrations.

4. Conclusions

In this work, an in-depth investigation of the influence of carbon nanotubes on the structural, thermal, electrophysical and mechanical properties of nanocomposites based on poly-lactic acid was carried out. It was shown that the introduction of CNTs does not lead to the formation of new chemical bonds, but substantially influences the degree of crystallinity of the polymer matrix. An uneven nature of the concentration dependence of crystallinity was revealed: the maximum at a content of 0.6% CNTs indicates their role as nucleating agents, whereas at higher concentrations, agglomeration of nanotubes is observed, which limits the mobility of polymer chains and reduces the degree of crystallinity.

DSC analysis of PLA-CNT systems confirmed changes in temperature characteristics with changes in the concentration of nanotubes. At low CNT contents (up to 0.5%), an increase in the melting temperature and degree of crystallinity is observed, which indicates the role of CNTs as crystallization centers. An increase in these parameters indicates an increase in the ordering of the polymer phase and stabilization of its thermal characteristics. However, when the concentration of nanotubes is exceeded, this effect is leveled out, probably due to the formation of agglomerates and disruption of the homogeneity of the structure, which negatively affects the thermal properties of the material. For PLA-CNT nanocomposites, typical percolation behavior of electrical conductivity was found with a percolation threshold of about 0.5%. This suggests the effective formation of electrically conductive channels in the polymer matrix when a critical concentration of CNTs is reached. After reaching the threshold value, the electrical conductivity increases by several orders of magnitude, which opens up the possibility of creating functional materials with electrical properties. This effect can be explained by the formation of a continuous spatial network of nanotubes, which ensures charge transfer throughout the volume of the composite. Mechanical tests revealed a complex relationship between tensile strength and elongation at break on the CNT content, with a minimum at filler content of 1%. This behavior is explained by the competition between the effects of nanotube agglomeration and the formation of a reinforcing network in the polymer matrix. The increase in strength at higher CNT

concentrations is due to the formation of a spatially interconnected structure with CNTs.

Thus, the results of the study emphasize the importance of controlling the content and dispersion of CNTs in the PLA matrix to optimize the physicochemical characteristics of nanocomposites and achieve a balance between their structural ordering, thermal stability, electrical conductivity and mechanical strength.

Acknowledgements

This work was carried out within the framework of the research project "Creation of multifunctional polymer nanocomposite materials reinforced with para-aramid fibres and carbon nanotubes, in which the relationship between their structure and properties is predicted and established", which is financed from the state budget by the Ministry of Education and Science of Ukraine. State registration number 0124U001739. The authors thank all brave defenders of Ukraine who allow us to continue our scientific work.

References

1. P. Purnama, Z.S. Saldi, M. Samsuri, *J. Compos. Sci.* **8**, 317 (2024). <https://doi.org/10.3390/jcs8080317>.
2. L. Pietrzak, G. Raniszewski, L. Szymanski, *Electronics*, **11**, 3180 (2022). <https://doi.org/10.3390/electronics11193180>.
3. E.A. Lysenkov, V.V. Klepko, *J. Nano- and Electronic Phys.* **8**, 01017 (2016). [https://doi.org/10.21272/jnep.8\(1\).01017](https://doi.org/10.21272/jnep.8(1).01017).
4. E.A. Lysenkov, V.V. Klepko, I.P. Lysenkova, *J. Phys. Stud.* **21**, 4701 (2017). <https://doi.org/10.30970/jps.21.4701>.
5. G. Burlak, G. Medina-Ángel, *Prog. Electromagn. Res. Lett.* **74**, 77 (2018). <https://doi.org/10.2528/PIERL17120407>.
6. A. Battisti, A.A. Skordos, I.K. *Compos. Sci. Technol.* **70**, 633 (2010). <https://doi.org/10.1016/j.compscitech.2009.12.017>.
7. I. Lakin, Z. Abbas, R.S. Azis, et al., *Materials*, **13**, 4581 (2020). <https://doi.org/10.3390/ma13204581>.
8. D. Mi, Z. Zhao, H. Bai, *Materials*, **16**, 4012 (2023). <https://doi.org/10.3390/ma16114012>.
9. E.A. Lysenkov, V.V. Klepko, Yu.V. Yakovlev, *J. Nano- and Electron. Phys.* **7**, 01031 (2015). https://jnep.sumdu.edu.ua/en/full_article/1447.
10. D. Wu, L. Wu, W. Zhou et al., *J. Polym. Sci. B Polym. Phys.* **48**, 479 (2010). <https://doi.org/10.1002/polb.21909>.

11. K.K. Wong, S.-Q. Shi, K.T. Lau, *Key Eng. Mater.* **334-335**, 705 (2007). <https://doi.org/10.4028/www.scientific.net/KEM.334-335.705>.
12. F.H. Likhi, M. Singh, H.R. Potdukhe, et al., *ACS Appl. Mater. Interfaces.* **16**, 57253 (2024). <https://doi.org/10.1021/acsami.4c16329>.
13. A.S. Zeraati, S.A. Mirkhani, U. Sundararaj, *J. Phys. Chem. C.* **121**, 8327 (2017). <https://doi.org/10.1021/acs.jpcc.7b01539>.
14. Q. Zhang, S. Zhang, *J. Mater. Sci. Chem. Eng.*, **10**, 30 (2022). <https://doi.org/10.4236/msce.2022.104003>.
15. F. Beltrán, H. Aksas, L. Salah et al., *Materials.* **16**, 5356 (2023). <https://doi.org/10.3390/ma16155356>.
16. E. Lysenkov, V. Klepko, *J. Eng. Phys. Thermo-phys.*, **88** 1008 (2015). <https://doi.org/10.1007/s10891-015-1278-3>.
17. R. Mohan, J. Subha, J. Alam, *Adv. Polym. Technol.* **37**, 256 (2016). <https://doi.org/10.1002/adv.21664>.
18. D. Perin, G. Fredi, D. Rigotti et al., *J. Appl. Polym. Sci.* **139**, 51740 (2022). <https://doi.org/10.1002/app.51740>.
19. B.W. Chieng, N.A. Ibrahim, W.M.Z.W. Yunus et al., *Polymers*, **6**, 93 (2014). <https://doi.org/10.3390/polym6010093>.
20. K.R. Abdul Mannana, K.R. Kazmi, M.S. Khan et al., *J. Sci. Ind. Res.* **49**, 72 (2006). <https://pjsir.org/multidisciplinary-archive/Volume%2049%202006/issue2-49.html>.
21. A.M. Gohn, J. Seo, R.H. Colby et al., *Polymer*, **199**, 122548 (2020). <https://doi.org/10.1016/j.polymer.2020.122548>.
22. E.A. Lysenkov, O.V. Stryutskiy, Yu.P. Gomza et al., *Funct. Mater.* **22**, 40 (2015). <https://doi.org/10.15407/fm22.01.040>.
23. P.H. da Silva Leite Coelho, M.S. Marchesin, A.R. Morales et al., *Mater. Res.*, **17**, 127 (2014). <https://doi.org/10.1590/S1516-14392014005000059>.
24. V.V. Klepko, E.A. Lysenkov, *Ukr. J. Phys.* **60** 944 (2015). <https://doi.org/10.15407/ujpe60.09.0944>.
25. P. Angelova, *J. Theor. Appl. Mech.* **49**, 241 (2019). <https://doi.org/10.7546/JTAM.49.19.03.04>.
26. L. Yang, S. Li, X. Zhou et al., *Synth. Met.* **253** 122 (2019). <https://doi.org/10.1016/j.synthmet.2019.05.008>.
27. A.F. Rifa'i, M. Kaavessina, S. Distantina, *Period. Polytech. Chem. Eng.* **69** 149 (2025). <https://doi.org/10.3311/PPch.37876>.